Quantitative determination of deformation by sliding wear

QUANTITATIVE DETERMINATION OF DEFORMATION BY SLIDING WEAR

J. H. DAUTZENBERG and J. H. ZAAT

Mechanical Engineering Materials Laboratory, University of Technology, Eindhoven (The Netherlands)

SUMMARY

On the basis of a model, equations have been derived to define for true shearing, the effective deformation from the deflection of the grain boundaries and from the change of grain thicknesses. A linear intercept method was developed for the direct measurement of grain thickness. The theory has been checked by sliding OFHC copper against steel SAE 1045 under conditions of true shearing. The theory may be applied to other processes besides wear where substantial deformation occurs.

INTRODUCTION

When two materials slide against each other under pressure without any lubricant substantial plastic deformation may occur at the mating surfaces[1,2]. In many instances the deformation can be excessive. In service such severe wear cannot be tolerated as worn parts have to be replaced. In this paper such deformation is analyzed in detail and methods are worked out for quantifying the deformation. Experiments based on the sliding couple OFHC copper against steel SAE 1045 (0.45% C) (copper as a pin, steel as a ring) show how the method works in practice; the wear conditions being chosen in such a way that displacement of copper mainly occurred. Macroscopic measurement of deformation using gratings applied to the specimen before test has been made[3]. After test, deformation can be determined from the rotation and displacement of the grating with respect to a fixed point[4]. However, this method is not suitable for measuring deformation which occurs in the course of the wear process as the depth of the region of gross deformation is usually very small (for Cu less than 300 μm) and the deformation is so severe that after test the grating would hardly be discernible. Also, deformation of the worn material is not uniform; it may vary considerably from point to point, even at equal distances from the surface whilst the application of a grating may influence the wear process. Deformation may be measured by the geometrical alteration of metal grains. The manner in which an ideal spherical grain deforms under the influence of true shearing[5] arising during severe wear and how the deformation may be related to grain dimensions and to the deflection of the grain boundaries has been derived.

MODEL OF TRUE SHEARING

Starting with ideal spherical crystals deforming under the influence of true shearing $d\gamma_{yx} \neq 0$:

$$d\delta_x = d\delta_y = d\delta_z = d\gamma_{zy} = d\gamma_{xz} = 0 \tag{1}$$

in which $d\delta_{x,y,z}$ signify the natural incremental normal strain components and $d\gamma_{ij}$ the shear strain components. According to the Lévy–von Mises equations[4,6] which hold in general:

$$d\delta_x = \frac{d\bar{\delta}}{\bar{\sigma}}\left(\sigma_x - \frac{\sigma_y + \sigma_z}{2}\right) \qquad d\gamma_{yx} = 3\frac{d\bar{\delta}}{\bar{\sigma}}\tau_{yx}$$

$$d\delta_y = \frac{d\bar{\delta}}{\bar{\sigma}}\left(\sigma_y - \frac{\sigma_z + \sigma_x}{2}\right) \qquad d\gamma_{zy} = 3\frac{d\bar{\delta}}{\bar{\sigma}}\tau_{zy} \tag{2}$$

$$d\delta_z = \frac{d\bar{\delta}}{\bar{\sigma}}\left(\sigma_z - \frac{\sigma_x + \sigma_y}{2}\right) \qquad d\gamma_{xz} = 3\frac{d\bar{\delta}}{\bar{\sigma}}\tau_{xz}$$

in which $\sigma_{x,y,z}$ signify the 3 normal stress components and τ_{ij} the shear stress components. The incremental effective plastic strain $d\bar{\delta}$ and the effective stress $\bar{\sigma}$ are defined as[4]:

$$\frac{9}{4}(d\bar{\delta})^2 = \frac{1}{2}[(d\delta_x - d\delta_y)^2 + (d\delta_y - d\delta_z)^2 + (d\delta_z - d\delta_x)^2] + \frac{3}{4}[d\gamma_{yx} + d\gamma_{zy}^2 + d\gamma_{xz}^2]$$
$$2\bar{\sigma}^2 = (\sigma_x - \sigma_y)^2 + (\sigma_y - \sigma_z)^2 + (\sigma_z - \sigma_x)^2 + 6\tau_{yx}^2 + 6\tau_{zy}^2 + 6\tau_{xz}^2 = 6k^2 \tag{3}$$

From eqns. (1) and (2) it follows that:

$$\sigma_x = \sigma_y = \sigma_z \qquad \tau_{zy} = \tau_{xz} = 0 \tag{4}$$

From eqns. (3) and (4) it follows that:

$$\bar{\sigma} = \tau_{yx}(3)^{\frac{1}{2}} = k(3)^{\frac{1}{2}} \qquad d\bar{\delta} = \frac{d\gamma_{yx}}{(3)^{\frac{1}{2}}} = \frac{1}{(3)^{\frac{1}{2}}}\frac{dl_x}{l_y} \tag{5}$$

Integration of eqn. (5) leads to:

$$\bar{\delta} = \frac{1}{(3)^{\frac{1}{2}}}\frac{1}{l_y}\int_0^{l_x} dl_x = \frac{1}{(3)^{\frac{1}{2}}}\frac{l_x}{l_y} = \frac{\text{tg }\gamma}{(3)^{\frac{1}{2}}} \tag{6}$$

in which γ = angle of shear under the influence of the shear stress and l_y = OA of Fig. 1. To determine $\bar{\delta}$ two quantities require to be measured with the aid of a microscope, viz., the deflection of the grain boundaries and the decrease of grain thickness.

DETERMINATION OF THE DEFORMATION FROM THE DEFLECTION OF THE GRAIN BOUNDARIES

Consider a cross-section of the material (Fig. 1) situated in such a way that it is both perpendicular to the plane of the shear stress and parallel to this shear stress. In such a cross-section a grain boundary (OCB) makes an angle ζ with the normal (OA) on the shear stress plane. By true shearing this grain boundary OCB transforms into OEF, in such a way that AB = DF.
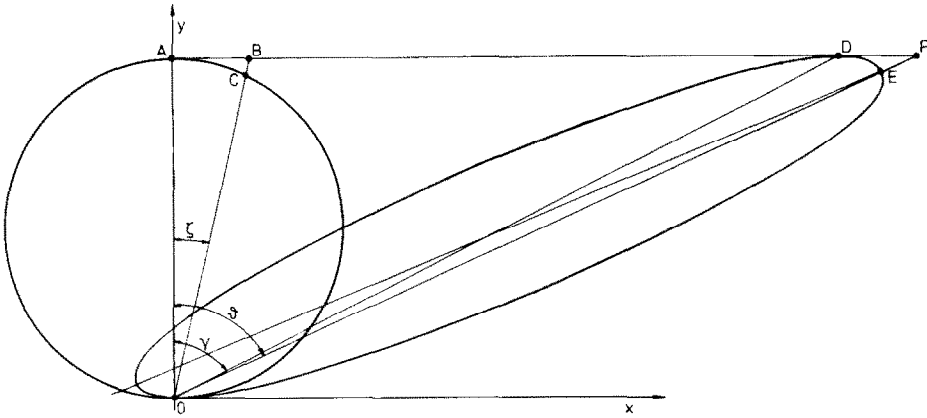
Fig. 1. Model for true shearing of a sphere.

Further angle $AOD = \gamma = $ angle of shear and angle $AOF = \theta = $ angle of the sheared boundary (OF) with the normal of the shear stress plane.

From geometrical considerations it follows:

$$\text{tg } \gamma = \text{tg } \theta - \text{tg } \zeta \tag{7}$$

or by eqn. (6)

$$\delta = \frac{\text{tg } \theta - \text{tg } \zeta}{(3)^{\frac{1}{2}}} = \left(1 - \frac{\text{tg } \zeta}{\text{tg } \theta}\right) \frac{\text{tg } \theta}{(3)^{\frac{1}{2}}} \tag{8}$$

Thus the effective deformation may be determined using eqn. (8). However, this method is not practicable for large values of δ since the direction of the grain boundary in the heavily deformed area cannot be determined; the second method is required.

DETERMINATION OF THE DEFORMATION FROM THE DECREASE IN GRAIN THICKNESS

With a spherical metal grain (radius $\frac{1}{2}D$) deformed as a result of a shear stress, consider the cross-section passing through the centre of the sphere and perpendicular to the plane of the shear stress. The spherical cross-section with centre $M(0, \frac{1}{2}D)$, Fig. 2, can then be expressed by the equation:

$$x^2 + \left(y - \frac{D}{2}\right)^2 = \frac{D^2}{4} \tag{9}$$

For true shearing over the angle γ,

$$x' = x + y' \text{ tg } \gamma$$
$$y' = y \tag{10}$$

in which x' and y' are the coordinates of the geometrical figure, arising from the circle by true shearing. Filled out in eqn. (9) this yields

$$x' + y'^2(1 + \text{tg}^2 \gamma) - 2x'y'\text{tg } \gamma - y'D = 0 \tag{11}$$

Introduction of a new orthogonal system of coordinates ξ, η with the centre $(\frac{1}{2}D \text{ tg } \gamma, \frac{1}{2}D)$ of the ellipse and rotated by an angle α (α being the angle between the largest mean
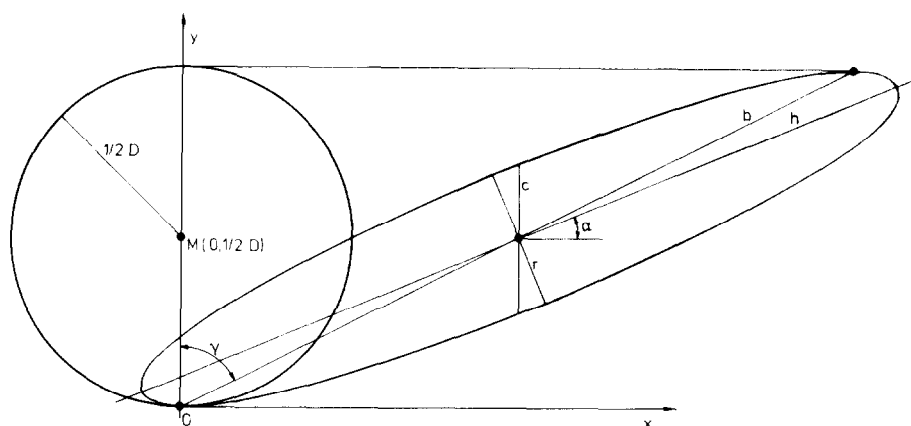
Fig. 2. Model for deformed metal grain.

axis of the ellipse and the x-direction) with respect to the original system x, y yields

$$\operatorname{tg} \gamma = \frac{1}{\operatorname{tg} \alpha} - \operatorname{tg} \alpha = \frac{2}{\operatorname{tg} 2\alpha} \tag{12}$$

and

$$r = D \operatorname{tg} \alpha; \quad h = \frac{D}{\operatorname{tg} \alpha} \tag{13}$$

The length of the chord passing through the centre of the ellipse and perpendicular to the x-axis can be derived by introducing the coordinates of the centre of the ellipse in eqn. (11). This becomes,

$$c = D \cos \gamma \tag{14}$$

Substituting eqn. (14) in eqn. (6) gives:

$$\bar{\delta} = \left[\frac{\dfrac{D^2}{c^2} - 1}{3} \right]^{\frac{1}{2}} \tag{15}$$

or, for $D \gg c$, this leads to

$$\bar{\delta} = \frac{D}{c(3)^{\frac{1}{2}}} \tag{16}$$

For the determination of c and D it is assumed that the section passes through the centre of the ellipse. However, in practice this is difficult to accomplish. Therefore c and D require to be determined indirectly by the linear intercept[7] method.

THE LINEAR INTERCEPT METHOD

Commencing again with spherical crystals, if this material is subjected to homogeneous shear only then is it possible to determine the average grain size from a section parallel to the x–y plane. Lines parallel to the y-axis are drawn on this section and where intersected by the grain circumference are called the linear inter-
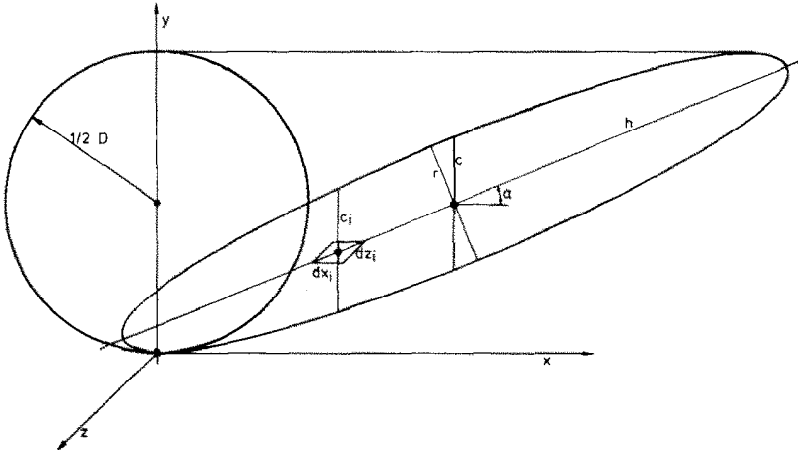
Fig. 3. Linear intercepts c_i.

cepts. It can be proved that the average linear intercept possesses a constant ratio to the smallest axis of the ellipsoid, arising from a sphere by true shearing (Fig. 3). A small surface element $dx_i dz_i$ is taken, (see Fig. 3) perpendicular to c_i ($c_i /\!/ c$). The angle between the largest main axis of the ellipse and the x-axis is equal to α. The volume V of the ellipsoid is:

$$V = \frac{4}{3} \frac{\pi r h D}{8} \tag{17}$$

where r, h and D are the main axes of the ellipsoid. Also,

$$V = \sum_{i=1}^{n} c_i \, dx_i dz_i \tag{18}$$

The projection of the little element $dx_i dz_i$ on the large ellipse determined by h and D amounts to:

$$\frac{dx_i dz_i}{\cos \alpha} \tag{19}$$

This is α as defined by eqn. (12)

Taking a large number of small but equal surface elements so that the large ellipse is complete, then using eqn. (19), eqn. (18) becomes:

$$\frac{dx_i dz_i}{\cos \alpha} \cdot \cos \alpha \sum_{i=1}^{n} c_i = V \tag{20}$$

where n is equal to the number of small elements. Then

$$\sum_{i=1}^{n} c_i = n\bar{c} \tag{21}$$

where $\bar{c} =$ average linear intercept. Further,

$$\frac{n\,dx_i\,dz_i}{\cos\alpha} = \frac{\pi D h}{4} \tag{22}$$

Substituting eqns. (22), (21) and (17) in eqn. (20) yields:

$$\bar{c}\cos\alpha = \tfrac{2}{3}r \tag{23}$$

and with eqns. (13) and (14), eqn. (23) becomes:

$$\bar{c}\cos\alpha = \frac{2}{3}\,D\,\mathrm{tg}\,\alpha = \frac{2}{3}c\,\frac{\mathrm{tg}\,\alpha}{\cos\gamma} \tag{24}$$

or with eqn. (12)

$$\bar{c} = \tfrac{2}{3}c(1 + \mathrm{tg}^6\,\alpha)^{\frac{1}{2}} \tag{25}$$

For $\alpha < \pi/8$ that is for $\gamma > \pi/3$ within an accuracy of 1%,

$$\bar{c} = \tfrac{2}{3}c \tag{26}$$

For a sphere the following equation holds strictly,

$$\bar{D} = \tfrac{2}{3}D \tag{27}$$

so eqn. (15) becomes,

$$\delta \simeq \left[\frac{\dfrac{\bar{D}^2}{c^2} - 1}{3} \right]^{\frac{1}{2}} \tag{28}$$

or for $\bar{D} \gg \bar{c}$

$$\delta = \frac{\bar{D}}{\bar{c}(3)^{\frac{1}{2}}} \tag{29}$$

where $\bar{c}$ and $\bar{D}$ are the average linear intercepts of the deformed and the original grains respectively.

PREPARATION OF THE SAMPLES AND EXPERIMENTAL SET-UP

The wear experiments were carried out using a controlled atmosphere pin ring apparatus with an OFHC copper pin and a normalized steel SAE 1045 ring (Fig. 4). Test conditions were chosen so that displacement of copper only occurred. The pins were cylindrical, 30 mm long and 8 mm diameter. To measure temperature during test the pin had an axial cylindrical hole, 20 mm long and 3.5 mm diameter, to hold a thermocouple. After machining all copper pins were annealed for three hours at 750°C in a vacuum of approximately 10^{-5} Torr.

The pins made complete contact with the disk when viewed macroscopically. The rings were flat disks of normalized steel 80 mm diameter and 10 mm thick. The rings were mounted on the apparatus so that the eccentricity of the ring in the radial direction with reference to the axis of rotation was less than 1 μm. Both ring and pin were ground and finally polished with 1 μm diamond paste. The apparatus was constructed so that the ring and pin were constantly in an argon atmosphere (O_2 content $\leqslant$ 30 p.p.m., water content $\leqslant$ 30 mg/m^3, or, $P_{O_2} < 3 \times 10^{-5}$ atm, $P_{H_2O} <$
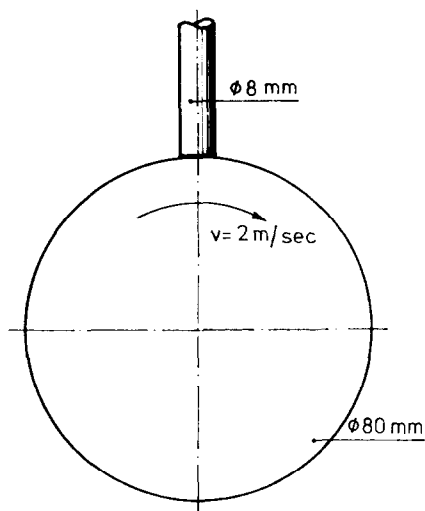
Fig. 4. Schematic arrangement of the pin–ring apparatus.

2×10^{-6} atm.). The pin was pressed against the ring with a force of 40 N. The peripheral speed of the ring was 2 m/sec ($= 50$ rad s^{-1}). During the test, friction, load, radial displacement of the pin (a measure of wear rate) and temperature were measured by a thermocouple connected intimately to the bottom of the hollow pin. After test, the pin was sectioned through the axis parallel to the sliding direction for microscopic investigation. After polishing and etching (ammonia with hydrogen peroxide) the deformed structure was observed with a light-microscope and photographed. Using a replica (silver–carbon–WO$_3$) the grain structure was photographed in the electron microscope. Lines perpendicular to the plane of the worn surface were drawn on the electron micrograph; the distance between the lines was approximately twice the grain thickness. From the chords formed by the intersection of these lines and the grain circumference, a c_i was obtained.

To reduce the number of measurements, bands of constant width were taken parallel to the contact surface, the effective deformation being assumed constant within such a band. The width of the bands was chosen so that at least 25 linear intercepts could be measured within one band. Using eqn. (21) the average linear intercept, $\bar{c}$, in each band was determined. For bands farthest from the surface the values of a pair of bands were combined to reduce the work. The $\bar{D}$ (average linear intercept of the original material) was also determined by electron microscopy. It was not possible to use the light microscope as not all the grain boundaries could be resolved. A cross-section of the ring (perpendicular to the wear plane and parallel to the direction of wear) was made. After etching with nital the structure was observed by electron microscopy using silver–carbon–WO$_3$ replicas. The effective deformation was determined from the deviation of the cementite lamellae using eqn. (8).

RESULTS AND DISCUSSION

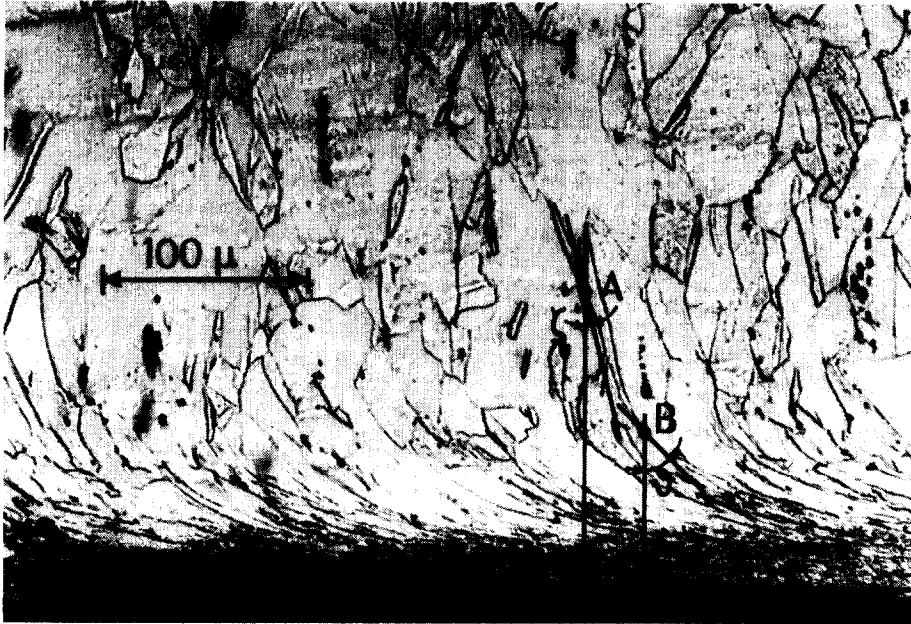(1) From the deviation of the grain boundaries in the copper (Fig. 5) and the
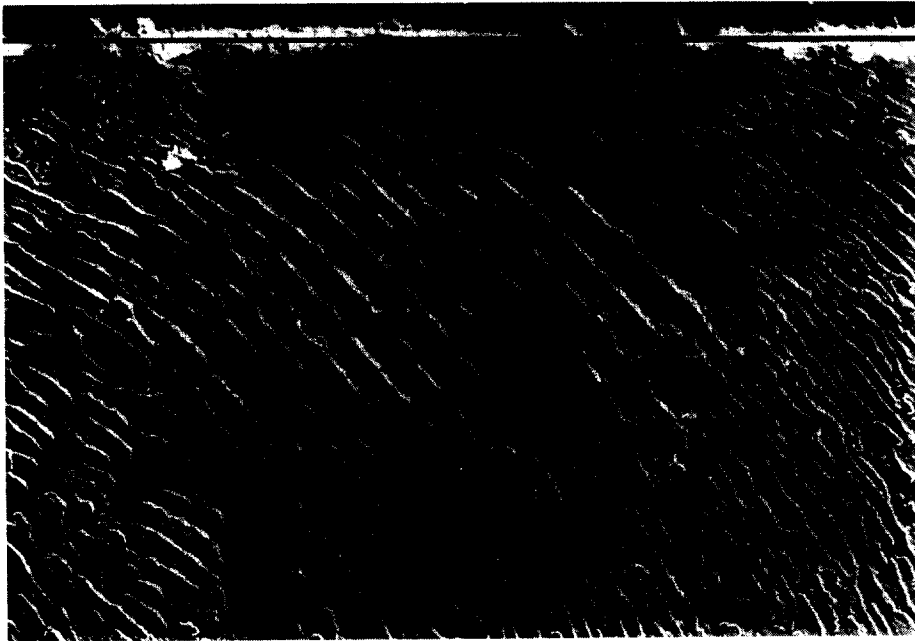
Fig. 5. Structure of deformed copper. (Photomicrograph, ×270)

Fig. 6. Structure of deformed SAE 1045 steel. (Electron micrograph, ×11,000)

cementite lamellae in the steel (Fig. 6) it is possible to determine ζ and θ, and using eqn. (8) the effective deformation in point B for copper and steel. The deviation may be determined unequivocally from a twin boundary (Fig. 5).

(2) Figure 5 shows clearly that nearly all the grain boundaries lying on the same straight line and at the same short distance from the contact surface make approximately the same angle with this plane. From eqn. (8) it may be derived that with high effective deformations, large variations of ζ have only a small influence on the effective deformation.

Figure 5 shows that all grain boundaries in the wear zone, equidistant from the surface, run parallel.

(3) Using eqn. (29) and applying the linear intercept method, from Fig. 7 the effective deformation can be determined at various distances from the contacting surface.
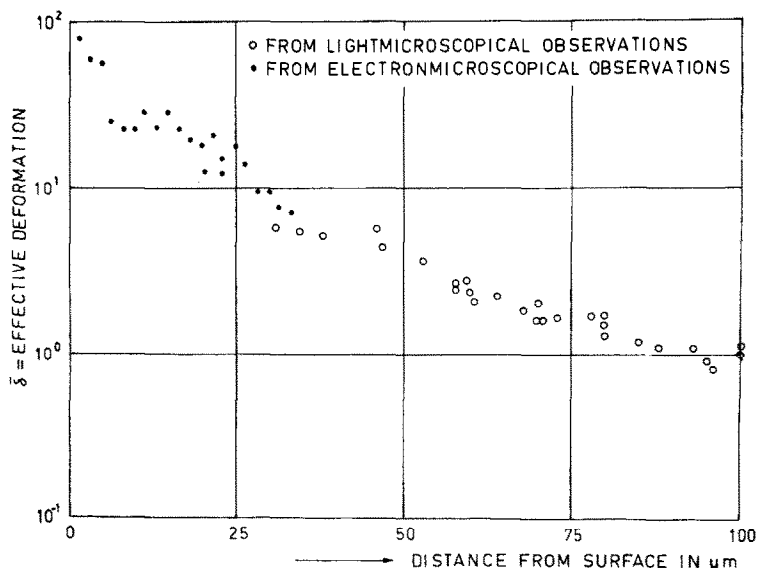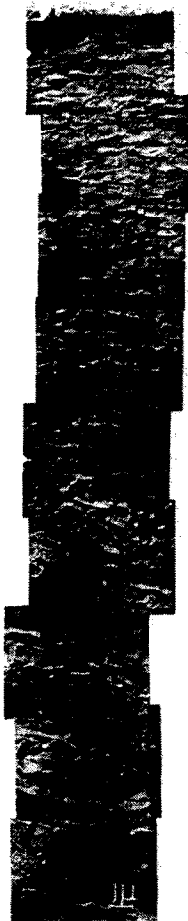

Fig. 7. Structure of deformed copper. (Electron micrograph, × 3000)

Fig. 8. Effective deformation of copper as a function of the distance from the sliding surface.

(4) Figures 5, 6, and 7 show that the effective deformation increases towards the surface. In copper the deformation is much greater than in steel.

(5) The depth of deformation field in steel is much less than in copper.

(6) Figure 7 shows that the grains are small towards the surface and the grain boundaries cannot be resolved by optical microscopy as previously found with the sliding of nickel on nickel[9].

(7) Figure 8 plots the effective deformation (δ) in copper as a function of distance from the surface. δ at the wear surface may reach very high values without rupture occurring. This may be understood if the load causes a hydrostatic pressure. We will elucidate this in a future publication[5].

(8) The bulk temperature of the copper measured at a distance of a few mm from the rubbing surface was approximately 120°C.

(9) The original grain size $\bar{D}$, determined electron microscopically was 10.2 μm. The problem of poor resolution of the optical microscope is overcome by using the electron microscope with a resolving power of better than 30 Å. A disadvantage is that more micrographs are necessary.

(10) Analytical considerations show that for $\gamma > \pi/3$ the error introduced by calculating the average linear intercept from the intercepts in the y-direction instead of in the direction of the smallest main axis of the ellipsoids is less than 1%.

CONCLUSIONS

(1) Using the model developed it is possible to determine the effective deformation in worn materials from optical and electron microscopical observations.

(2) Deformation in the worn surface may reach high values of $\delta = 10^2$.

(3) Very small average grain sizes (0.13 μm) are found near the surface.

(4) The original grain size should be determined in such a way, that on increasing the resolving power of the microscope, the grain size does not diminish.

(5) With the aid of the linear intercept method it is possible to determine the average grain size from a cross-section of a metallic material.

(6) The model may also be used with ellipsoid shaped grains; the same formulae for the effective deformation are derived.

(7) Contrary to Hensler[7] it was found that the ratio of average linear intercept and grain size is equal to $2:3 = 0.67$.

ACKNOWLEDGEMENT

REFERENCES

1 I. V. Kragelskii, *Friction and Wear*, Butterworths, London, 1965, p. 145.

2 L. Gümbel, *Reibung und Schmierung im Maschinenbau*, Verlag von M. Krayn, Berlin, 1925.

3 J. H. Zaat, Methode voor het aanbrengen van een lijnennetwerk op metaaloppervlakken, *Metalen*, 12 (19) (1957).

4 E. Thomson, C. Yang and S. Kobayashi, *Mechanics of Plastic Deformation in Metal Processing,* The Macmillan Co., New York, 1965.
5 J. H. Dautzenberg and J. H. Zaat, *Wear,* to be published.
6 P. C. Veenstra, Grondslagen van de mechanische technologie, *Technische Plasticiteitsleer,* Technische Hogeschool Eindhoven.
7 J. H. Hensler, The relation between grain section and grain size, *J. Inst. Metals,* 96 (1968) 190–192.
8 D. Landheer, Enkele verbeteringen aan de grote slijtageapparaten. *Internal Report WM-11-A-8,* Werktuigkundige Materialenkunde, Technische Hogeschool Eindhoven.
9 G. T. Newman, O. D. Smith, D. K. Matthes and C. R. Brooks, Application of electron microscopy to the study of surface topography and subsurface microstructure in wear, *U.S. Navy Contract N 00014-68-A-0144,* Knoxville, Tennessee.